

Unoccupied d states of Au impurities in silicon as studied by x-ray-absorption spectroscopy

Z. H. Lu, T. K. Sham, M. Vos, A. Bzowski, I. V. Mitchell, and P. R. Norton

Interface Science Western and Departments of Chemistry and Physics, University of Western Ontario, London, Ontario, Canada N6A 5B7

(Received 16 April 1991; revised manuscript received 27 December 1991)

Samples of n -type Si(111) were ion implanted with 10^{16}-cm^{-2} Au^+ ions at 1 MeV energy, and were then annealed using the rapid-thermal annealing method. Total-electron-yield Au $L_{2,3}$ edge x-ray-absorption spectroscopy was used to study the d -orbital structures of a Au atom when it is incorporated into the Si lattice. From near-edge absorption studies, we found that the "white-line" areas, relative to bulk Au, of both as-implanted and annealed samples have been significantly increased. The results show that d electrons are depleted when Au interacts with silicon. The estimated Au d -orbital configuration is $d^{9.75-\delta}$ in ion-amorphized Si, and is $d^{9.89-\delta}$ in recrystallized Si. (δ is the bulk Au d -hole number.) This provides experimental evidence that the d shell of Au impurities does not have the full complement of ten electrons.

It is well known that Au impurities produce two deep levels in the band gap of silicon,^{1,2} and this has been used to control the carrier lifetime in various devices.² Au in silicon is known to occupy either a substitutional or an interstitial site. For the interstitial site, the orbital overlap between Au and the surrounding Si atoms is thought to be very weak, and the Au behaves like a free atom with closed d^{10} shell.³ For a substitutional Au atom, a strong interaction with four nearest Si dangling sp^3 orbitals is expected. Many models have been proposed to interpret the electronic states of a substitutional Au. From a chemical bonding point of view, all these models can be summarized as "open-shell" or "closed-shell" models. In the closed-shell model, the Au $5d$ orbital is considered as a closed shell with its full complement of ten electrons (d^{10}), without any participation in chemical bonding with neighbor silicon atoms. One typical example in this closed-shell category is the "vacancy" model proposed by Watkins.⁴ This vacancy model suggests that a Au atom, with a completely filled d^{10} shell, is located at a negatively charged vacancy. This seems to be substantiated by the calculation by Alves and Leite⁵ using the Watson-sphere-terminated cluster model. The open-shell model was proposed by Fazzio, Caldas, and Zunger.³ Based on calculations using a quasiband crystal-field Green's-function method, Fazzio, Caldas, and Zunger find that the substitutional Au d shell is not completely filled with electrons and the effective orbital configuration of the neutral impurity Au is $s^{0.3}p^{0.65}(dfg)^{9.54}$. However, neither of the above two models have been confirmed by any experiment. In this paper, we present our experimental measurement of the unoccupied $5d$ state in Au^+ -implanted silicon by x-ray-absorption spectroscopy, which include x-ray-absorption near-edge structure (XANES) and extended x-ray-absorption fine structure (EXAFS).

The "white line" absorption near the $L_{2,3}$ absorption edge is known to be primarily due to the x-ray-induced dipole transition of $p_{1/2}$ electrons to the unfilled portion of $d_{3/2}$ orbitals (L_2 edge), and of $p_{3/2}$ electrons to the unfilled portion of $d_{3/2,5/2}$ orbitals (L_3 edge).^{6,7} For a Au atom with a filled d^{10} shell, there should be no white line at $L_{2,3}$

edge. This technique has been successfully used to study the d charge transfer of a Au atom when it interacts with other constituent atoms in a Au compound.⁸⁻¹⁰

The x-ray-absorption experiment was conducted at the C2 beam line of the Cornell High Energy Synchrotron Source (CHESS). The Au $L_{2,3}$ absorption is measured through a total electron yield mode using a gas-flow electron detector.¹¹ The detector is designed in such a way that the silicon substrate can be rotated to diminish x-ray-diffraction effects. An n -type $1-3-\Omega\text{ cm}$ Si(111) sample was implanted with 10^{16}-cm^{-2} gold ions at 1-MeV ion energy, using the University of Western Ontario Tandem Accelerator. The depth distribution of Au is about 3000 Å, as measured by Rutherford backscattering (RBS), shown in Fig. 1. Some of the samples were then annealed using a commercial rapid thermal annealing (RTA) apparatus (heat pulse 410) for 15 s at 900°C. Raman spectroscopy measurements show that the as-implanted silicon

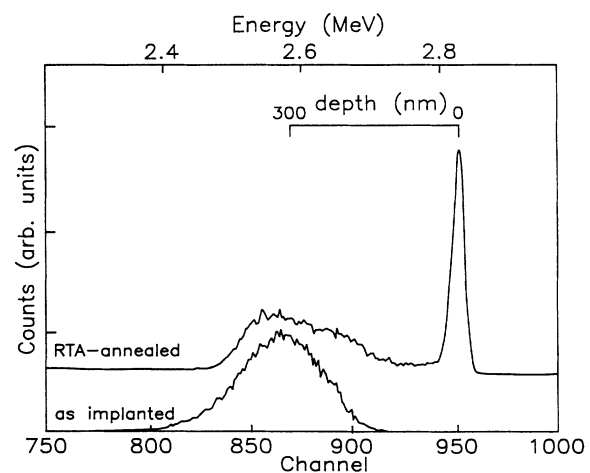


FIG. 1. RBS-measured Au distributions in as-implanted and 900°C RTA-annealed Si(111) samples. The measurement was carried out with 3-MeV He^+ ions at a backscatter angle of 110° .

is amorphous, while the RTA-annealed silicon was completely recrystallized. After RTA annealing, about 30% of the Au has segregated to the surface, as determined by the RBS measurement shown in Fig. 1.

In Fig. 2, we show the normalized Au L_3 -absorption spectra of as-implanted (dotted line), RTA-annealed (dashed line), and bulk Au (solid line). The spectra were normalized to the height of the edge jump. Photon energies were calibrated with the point of inflection of the Au L_3 -edge jump of pure Au at 11919 eV without further alignment. This procedure was based on our previous observation that the maximum Au core-level shift of Au in Si relative to pure Au is only 0.6 eV. This shift is qualitatively insignificant in this analysis as far as the alignment of Fermi level is concerned for two reasons: (1) the unoccupied d states are not exactly localized at the Fermi level³ and (2) the lifetime of the Au L_3 hole is about 8 eV. The shaded region indicates the white line absorption relative to bulk Au, which already has a weak white line, i.e., the presence of unoccupied states in the Au d band (d hole). From the figure, one notices the significant increase in white line intensity (i.e., d -hole population) in Au⁺ implanted, as well as RTA-annealed silicon samples relative to bulk Au. The same trend in white line absorption is also observed at L_2 -edge absorption and is shown in Fig. 3.

Using a relativistic tight-binding calculation, Mattheiss and Dietz¹² related the integrated white line absorption coefficient $A_{2,3}$ (subscripts indicate L_2 or L_3 edge) to d -hole population $h_{3/2,5/2}$ (subscripts indicate spin-orbit split $d_{3/2}$ or $d_{5/2}$) through

$$A_2 = C' N_0 \hbar \omega_2 (R_d^{2P_{1/2}})^2 h_{3/2}/3, \quad (1a)$$

$$A_3 = C' N_0 \hbar \omega_3 (R_d^{2P_{3/2}})^2 (6h_{5/2} + h_{3/2})/15, \quad (1b)$$

where $C' = 4\pi^2 a/3$ (a is the fine-structure constant), N_0 is the density of Au atoms, $\hbar \omega_{2,3}$ is the absorption edge energy, and $R_d^{2P_{3/2,5/2}}$ is the radial dipole-moment integral. If we assume $R_d^{2P_{3/2}} = R_d^{2P_{1/2}} = R_d^{2P}$, then we can derive the relation between the d -hole number $\Delta h_{3/2,5/2}$ relative to bulk Au and the white lines area $\Delta A_{2,3}$ (shaded region in

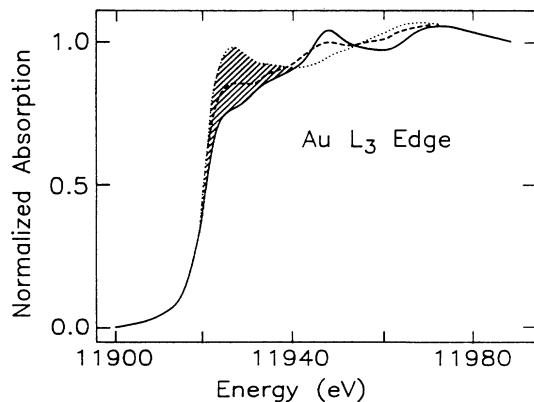


FIG. 2. Normalized Au L_3 -edge absorption spectra of as-implanted Au in silicon (dotted line), 900°C annealed (dashed line), and polycrystalline Au (solid line). The shaded area indicates the “white lines” absorption.

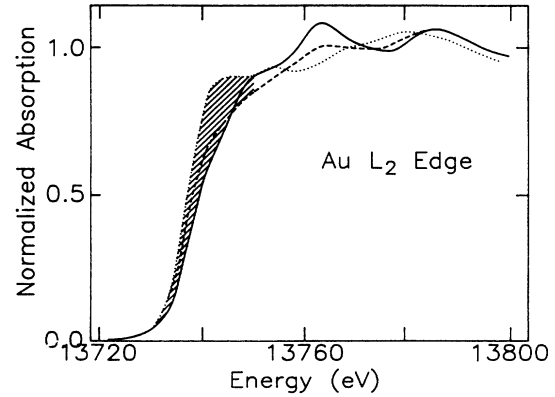


FIG. 3. Normalized Au L_2 -edge absorption spectra of as-implanted Au in silicon (dotted line), 900°C annealed (dashed line), and polycrystalline Au (solid line). The shaded area indicates the “white lines” absorption.

Figs. 2 and 3) relative to bulk Au

$$\Delta h_{3/2} = 3\Delta A_2/C, \quad (2a)$$

$$\Delta h_{5/2} = \frac{1}{2C} \left[\frac{5\hbar\omega_2}{\hbar\omega_3} \Delta A_3 - \Delta A_2 \right], \quad (2b)$$

where $C = C' N_0 \hbar \omega_2 (R_d^{2P})^2$. If we use the dipole transition value of platinum¹² $R_d^{2P} = 3.103 \times 10^{-11}$ cm, the Au atomic density $N_0 = 5.89 \times 10^{22}$ atoms cm^{-3} , the L_2 -edge energy of 1.37×10^4 eV, we then get $C = 7.46 \times 10^4$ eV cm^{-1} . $\Delta A_{2,3}$ can be obtained by multiplying the integrated area difference, from 10 eV below the edge to 15 eV above the edge of the normalized spectra, by $\Delta\sigma_{2,3}\rho$. The $\Delta\sigma_{2,3}$ are the photoabsorption cross-section differences above and below the absorption edge, and are 105.3 $\text{cm}^2 \text{g}^{-1}$ (Au L_3 edge)¹³ and 50.7 $\text{cm}^2 \text{g}^{-1}$ (Au L_2 edge), respectively. ρ is the density of Au, 19.3 g cm^{-3} . The values of $\Delta A_{2,3}$, together with derived d -hole number are given in Table I. The total d -hole number Δh of impurity Au in silicon, relative to bulk Au, is simply a sum of the $\Delta h_{3/2}$ and $\Delta h_{5/2}$. According to Mattheiss and Dietz¹², the d -hole number of pure Au is 0.401. We then get the absolute hole number h ($=\Delta h + 0.401$) of the Au impurities in silicon. All these values are given in Table I.

From the above experiments, it is clear that the Au d electrons are depleted when it interacts with silicon. This clearly favors the open-shell model. This experimental finding is not totally unexpected. From studies of Au-

TABLE I. Relevant parameters derived from Au $L_{2,3}$ XANES analysis.

Sample	White-lines area ($10^4 \text{ cm}^{-1} \text{ eV}$)		d -hole number			
	ΔA_2	ΔA_3	$\Delta h_{3/2}$	$\Delta h_{5/2}$	Δh	h
Si(Au)						
as implanted	0.234	0.427	0.094	0.156	0.25	0.65
Si(Au)						
RTA annealed	0.069	0.224	0.028	0.082	0.11	0.51

metalloid compounds such as AuAl₂ and AuGa₂, Sham *et al.*⁸ have observed a comparable amount of *d*-electron depletion in Au. The depletion of Au *d* electron, in the case of interaction between Au and Si(100) surface dangling bond, was also observed by Lu *et al.*¹⁴ using synchrotron radiation photoemission spectroscopy.

As to the geometric structure of Au in the as-implanted silicon, i.e., amorphous silicon, no sign of Au-Au bonds (i.e., in a Au cluster) has been found from EXAFS spectra analysis. This is not surprising. It is known¹⁵ that the solubility of Au is about approximately 6 orders of magnitude higher in amorphous than crystalline Si. Even at a dose of $2 \times 10^{17} \text{ cm}^{-2}$ of 2-MeV Au⁺-implanted amorphous silicon, no Au precipitation has been observed.¹⁵ Since the "free" interstitial Au with a closed *d*¹⁰ shell will not exhibit a significant white line, the white line observed must be from Au atoms which have some kind of chemical bonding with nearby silicon dangling bonds, which are abundant in amorphous silicon. It is well established that an amorphous silicon continuous random network has a well-defined first shell of four silicon atoms,¹⁶ and has a short-range or even medium-range tetrahedral topological arrangement. It is not unreasonable to assume that the Au impurities that produce the white line are located at tetrahedral substitutional sites, resembling its crystalline counterpart. The corresponding EXAFS of Fig. 3 supports this view qualitatively although the EXAFS data have larger uncertainty due to a poorer signal-to-noise ratio. Figure 4 shows the Fourier transform (FT) of the Au *L*₃ EXAFS with *k* weighting of pure Au, Au in Si as implanted, and after annealing at 900°C. *k* weighting places the emphasis on the Si backscatterers of the implanted samples since Si has large backscattering amplitude at the low-*k* region where the amplitude for Au is small. Figure 4(a) exhibits radial distribution of the first and second shell characteristic of pure Au peaking at 2.2 and 3.1 Å, respectively. These features are replaced by two peaks at 1.4 and 2.0 Å in the as-implanted sample [Fig. 4(b)]. The radial distance of the first peak (at 1.4 Å) is too short to be a Au-Si or Au-Au bond length and is attributed to an artifact due to high-*k* noise. The peak at 2.0 Å is shorter than expected for pure Au [Fig. 4(a)]. This, together with the absence of a 3.0-Å peak in Fig. 4(b) suggests that there is no significant Au clustering and the peak at 2.0 Å in the FT is dominated by Si backscattering. Assuming this is the case, we obtained a Au-Si bond distance of 2.48(5) Å by fitting the experimental phase derived from the filtered backtransform of the FT peak at 2.0 Å (with a 1.4–2.6 Å symmetric window) using theoretical phase shifts of Mckale *et al.*¹⁷ This value, despite its large uncertainty (arising primarily from static disorder), is in qualitative accord with the theoretical value of 2.52 Å, which is obtained by the sum of the Si tetrahedral radii¹⁸ of 1.17 Å and of the Au Bragg-Slater covalent radii¹⁹ of 1.35 Å. A comparable Au-Si bond length of 2.46 Å was also reported by Sawicki, Hitchcock, and Tyliczszak,²⁰ who used the same EXAFS analysis technique of 100-KeV Au⁺-implanted Si(111) at doses around 10^{16} cm^{-2} .

For the RTA-annealed sample (i.e., recrystallized silicon) we find that the white line area, relative to bulk Au,

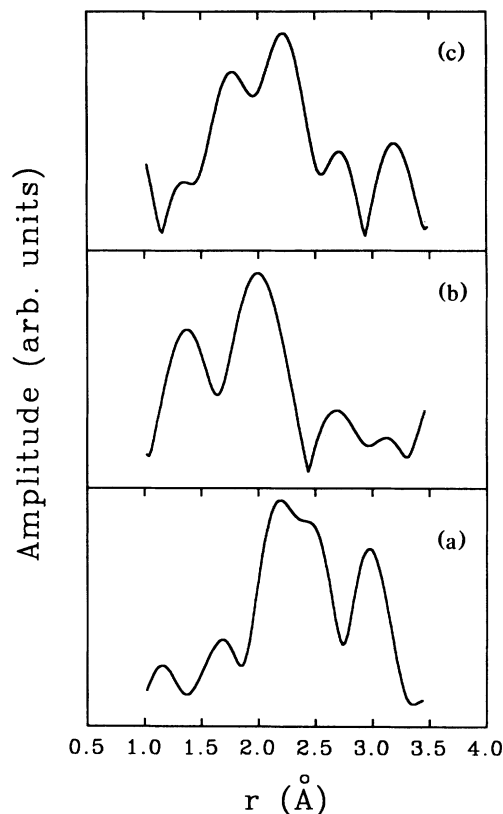


FIG. 4. Fourier transform of EXAFS ($k = \sim 3 - 10.5 \text{ \AA}^{-1}$) with *k* weighting for (a) pure Au, (b) Au implanted in Si, and (c) after annealing at 900°C. Maximum amplitudes are 2.8, 2.5, and 2.6 in (a), (b), and (c), respectively.

has been reduced by about 50%, as compared to the as-implanted sample. The near-edge structure grows more similar to bulk Au (see Figs. 2 and 3). This suggests the existence of Au clusters in the annealed sample.^{21,22} The cause of the reduction in white line area may be attributed to (1) increased numbers of interstitial Au and (2) formation of Au clusters. The EXAFS of the annealed sample is more complex and cannot be analyzed with confidence by a simple FT analysis. It almost certainly has multiphase contributions (Fig. 1). Detailed analysis requires careful modeling and better EXAFS data, and is not attempted here. Qualitatively, the results suggest that the Au-Si bond gets a little longer after annealing if we again assume that the Si backscatterers play a dominated role in the low-*k* region of the EXAFS.

From the above experiment, we can conclude that an open-shell model is the only model that can correctly describe the *d*-shell charge distribution. This is $d^{9.57}$ for a neutral substitutional Au⁰, according to Fazzio, Caldas, and Zunger.³ The semiquantitative values of *d*-shell charges derived from our near-edge white line absorption measurement are $d^{9.75-\delta}$ and $d^{9.89-\delta}$ for Au in as-implanted (amorphous) and RTA-annealed (crystalline) Si, respectively. δ is the bulk *d*-hole number, which is equal to 0.401, according to Ref. 12. The actual *d*-hole number for a substitutional Au may even be higher had we exclud-

ed the absorption by interstitial and cluster Au. The Au-Si bond length in amorphous silicon deduced from EXAFS is 2.48(5).

From $L_{2,3}$ -edge x-ray-absorption measurements, we cannot deduce any information about the Au 6(*sp*) charge distribution. However, from previous Mössbauer isomer shifts²³ of 3.3 mms^{-1} of dilute Au in Si, we find²⁴ that a Au 6s orbital actually gains 0.28 electron, instead of losing 0.7 electron as predicted by Fazzio, Caldas, and Zunger.³ This suggests that the current understanding of

noble-metal impurity electronic structures in silicon is still far from complete.

We wish to express our thanks to Dr. A. P. Hitchcock and Dr. T. Tyliczszak of the McMaster University for lending us the gas-flow electron detector, also to the CHESS staff for much technical assistance. This work is funded by NSERC (Canada) and OCMR (Ontario). CHESS is supported by the U.S. National Science Foundation.

¹W. M. Bullis, *Solid-State Electron* **9**, 143 (1966).

²See, for example, S. M. Sze, *Physics of Semiconductor Devices*, 2nd ed. (Wiley, New York, 1981).

³A. Fazzio, M. J. Caldas, and A. Zunger, *Phys. Rev. B* **32**, 934 (1985).

⁴G. D. Watkins, *Physica B* **117 & 118**, 9 (1983).

⁵J. L. A. Alves and J. R. Leite, *Phys. Rev. B* **30**, 7284 (1984).

⁶M. Brown, R. E. Peierls, and E. A. Stern, *Phys. Rev. B* **15**, 738 (1977).

⁷A. N. Mansour, J. W. Cook, Jr., and D. E. Sayer, *J. Phys. Chem.* **88**, 2330 (1984).

⁸T. K. Sham, *Solid State Commun.* **64**, 1103 (1987); T. K. Sham, Y. M. Yiu, M. Kuhn, and K. H. Tan, *Phys. Rev. B* **41**, 11881 (1990).

⁹F. W. Lytle, *Phys. Chem.* **91**, 1251 (1987).

¹⁰Y. Joen, N. Jisrawi, G. Liang, F. Lu, M. Croft, W. L. McLean, D. L. Hart, N. G. Stoffel, J. Z. Sun, and T. H. Geballe, *Phys. Rev. B* **39**, 5748 (1989); Y. Jeon, B. Qi, F. Lu, and M. Croft, *Phys. Rev. B* **40**, 1538 (1989).

¹¹T. Tyliczszak and A. P. Hitch, *Physica B* **158**, 335 (1989).

¹²L. F. Mattheiss and R. E. Dietz, *Phys. Rev. B* **22**, 1663 (1980).

¹³W. H. McMaster, N. Kerr Del Grande, and J. H. Hubell, *Compilation of X-Ray Cross Sections* (National Technical Information Service, Springfield, VA, 1969).

¹⁴Z. H. Lu, T. K. Sham, K. Griffiths, and P. R. Norton, *Solid*

State Commun. **76**, 113 (1990).

¹⁵J. K. N. Lindner, N. Hecking, and E. de Kaat, *Nucl. Instrum. Methods Phys. Res. Sect. B* **26**, 551 (1987).

¹⁶S. R. Elliott, *Physics of Amorphous Materials* (Longman, London, 1983).

¹⁷A. G. McKale, B. W. Veal, A. P. Paulikas, S. K. Chan, and G. S. Knapp, *J. Am. Chem. Soc.* **11**, 3763 (1988).

¹⁸J. C. Phillips, *Bonds and Bands in Semiconductors* (Academic, New York, 1973), p. 22.

¹⁹J. C. Slater, *Symmetry and Energy Bands in Crystals* (Dover, New York, 1972), p. 55.

²⁰J. A. Sawicki, A. P. Hitchcock, and T. Tyliczszak, *Physica B* **158**, 681 (1989).

²¹A. Balena and S. Mobilio, *J. Phys. (Paris) Colloq.* **12**, C8-1009 (1986).

²²A. Bianconi, *Synchrotron Radiation in Chemistry and Biology I*, Topics in Current Chemistry Vol. 145 (Springer-Verlag, Berlin, 1988), p. 56.

²³P. H. Barrett, R. W. Grant, M. Kaplan, D. A. Keller, and D. A. Shirley, *J. Chem. Phys.* **39**, 1055 (1963).

²⁴The isomer shift is 12 $\text{mms}^{-1} \Delta n_s$ (*s*-electron flow); see T. K. Sham, R. E. Watson, and M. L. Perlman, in *Advances in Chemistry*, edited by J. G. Stevens and G. K. Shenoy (American Chemical Society, Washington, DC, 1981), Vol. 194, p. 39.